Title

Chlorogenic acid combined with epigallocatechin-3-gallate mitigates d -galactose-induced gut aging in mice

Journal

Food & Function, 14(6)

ISSN

2042-6496

Authors

Wei, Ran
Su, Zhucheng
Mackenzie, Gerardo G

Publication Date

2023-03-20

DOI

10.1039/d2fo03306b

Chlorogenic acid combined with Epigallocatechin-3-Gallate mitigates D-galactose-induced gut aging in mice

Ran Wei[1], Zhucheng Su[1,*], Gerardo G. Mackenzie[2,*]

[1]Department of Tea Science, Zhejiang Agriculture and Forestry University, Hangzhou, 311300, China.

[2]Department of Nutrition, University of California, Davis, California, 95616, USA

*Corresponding authors:

Dr. Zhucheng Su, Ph.D.

Department of Tea Science, Zhejiang Agriculture and Forestry University

Hangzhou, Zhejiang, 311300, China

Phone: (0571) 63743302

E-mail: zhuchengsu@zafu.edu.cn

Dr. Gerardo G. Mackenzie, Ph.D.

Department of Nutrition, University of California, Davis

One Shields Ave. Davis, CA, 95616

Phone: (530) 752-2140; Fax: (530) 752-8966;

E-mail: ggmackenzie@ucdavis.edu

Running title: Chlorogenic acid plus EGCG ameliorates D-galactose-induced gut aging

Abstract

Chlorogenic acid (CGA) and Epigallocatechin-3-Gallate (EGCG) are major polyphenolic constituents of coffee and green tea with beneficial health properties. In this study, we evaluated the gut protecting effect of CGA and EGCG, alone or in combination, on D-galactose-induced aging mice. CGA plus EGCG more effectively improved the cognition deficits and protected the gut barrier function, compared to either agent alone. In particular, CGA plus EGCG prevented the D-galactose mediated reactive oxygen species accumulation by increasing the total antioxidant capacity, reducing the levels of malondialdehyde, and suppressing the activity of the antioxidant enzymes superoxide dismutase and catalase. In addition, supplementation of CGA and EGCG suppressed gut inflammation by reducing the levels of the proinflammatory cytokines TNFα, IFNγ, IL-1β and IL-6. Moreover, CGA and EGCG modulated the gut microbiome altered by D-galactose. For instance, CGA plus EGCG restored the *Firmicutes/Bacteroidetes* ratio of the aging mice to control levels. Finally, CGA plus EGCG decreased the abundance of *Lactobacillaceae*, *Erysipelotrichaceae*, and *Deferribacteraceae*, while increased the abundance of *Lachnospiraceae*, *Muribaculaceae*, and *Rikenellaceae*, at the family level. In conclusion, CGA in combination with EGCG ameliorated the gut alterations induced by aging, in part, through antioxidant and anti-inflammatory effects, and by modulating the gut microbiota.

Keywords: chlorogenic acid, EGCG, aging, oxidative stress, inflammation, microbiota dysbiosis

1. Introduction

Aging is characterized by a progressive decline in individuals' adaptability, physiological deterioration, and cognitive decline. Aging is also generally considered as a primary risk factor for developing various diseases, such as neurodegenerative disease, cardiovascular disorder, cancer, and diabetes[1]. It is estimated that in 2030, one-fifth of the population will be aged older than 65, which will increase the health care burden for families and governments[2]. Therefore, efforts to develop evidence-based anti-aging strategies are ongoing, including genetic, drugs, specific dietary interventions, and exercise.

Besides cognitive decline, which is a major problem during aging[3], the gut also undergoes critical changes with advanced age. For example, gut barrier function degenerates with aging, which plays key role in gut permeability and protecting gut health[4]. Increase in oxidative stress is observed in aging and it contributes to "leaky gut". Overproduction of reactive oxygen species (ROS) drives proinflammatory shift, which feeds back more ROS generation. This vicious cycle causes gut dysbiosis and increases gut permeability. In turn, the disruption of gut barrier facilitates translocation of endotoxin, which is highly involved in initiating the low-grade inflammation[5]. Though aging is an irreversible and inevitable process, the rate of aging can be controlled. Studies suggest that polyphenolic compounds have potential in slowing aging. In particular, this health beneficial effect is mediated, in part, by attenuating oxidative stress, suppressing inflammation, preventing of telomere attrition, modulating cell apoptosis, and restricting caloric intake[6].

Epigallocatechin-3-Gallate (EGCG) and chlorogenic acid (CGA) are the most abundant and active polyphenol components present in green tea and coffee, two of the most consumed beverages worldwide. For instance, a single cup of green tea contains about 200-300 mg of EGCG, an amount that has been documented to have health beneficial effects against various chronic diseases and aging[7]. On the other hand, CGA is widely distributed in plants and accounts up to 3% (w/w) of the roasted coffee powder[8]. In previous studies, EGCG and CGA have shown extensive health

promoting activities, such as anti-oxidation, anti-diabetes, and anti-cancer effects. In addition, extensive evidence have shown that EGCG and CGA perform well in anti-aging, including improving cognitive decline, relieving vascular senescence, and preventing skin photoaging[9-11]. In combination, it is reported that EGCG plus CGA display amplifying effect in preventing age-related bone loss, compared with each agent alone[12, 13]. However, it remains unknown whether EGCG and CGA, alone or in combination, could exert stronger protective effect against the aging gut.

In the present study, we assessed whether CGA and EGCG, alone or in combination, could ameliorate gut aging induced by D-galactose. D-galactose is a widely established aging model, which features cognitive dysfunction, memory loss, and motor degeneration[14]. Excess accumulation of D-galactose is easily reduced and catalyzed into nondegradable galactitol, which then interacts with amino acids and decreases the activity of the electron transport chain. Consequently, overproduction of advanced glycation end products (AGEs) and ROS accumulate with resulting increased oxidative stress and inflammation[15]. Moreover, long term D-galactose treatment could also damage gut integrity and lead to gut microbial dysbiosis[16]. In this study, we observed that the combination of CGA and EGCG attenuates D-galactose induced chronic gut injury, and this protection is mediated, in part, by their antioxidant and anti-inflammatory activities as well as the modulation of the gut microbiome.

2. Materials and Methods

2.1 Materials and Chemicals

Chlorogenic acid (purity≥98%) and EGCG (purity≥98%) were purchased from Solarbio (Beijing, China). D-galactose (purity≥98%) was purchased from Aladdin (Shanghai, China). The Elisa kits for TNFα, IFN-γ, IL-6 and IL-1β were purchased from Multisciences Biotech (Hangzhou, China). The ReverTra Ace qPCR RT master mix and the SYBR Green Realtime PCR master mix were purchased from TOYOBO (Shanghai, China). The designed oligo nucleotide primers were generated by Sangon Biotech (Shanghai, China). The RIPA lysis buffer, Halt protease inhibitor cocktail, 5×SDS-PAGE sample loading buffer, BSA, Bradford protein assay kit and ECL Plus

Ultra-Sensitive kit were purchased from Phygene (Haixi, China). The PVDF membranes and the fluorescein isothiocyanate-dextran (FITC-Dextran) were purchased from MilliporeSigma (Burlington, MA, USA). The endotoxin quantitation kit, the prestained protein ladder, and the TRIzol™ Reagent were purchased from Thermo Fisher Scientific (Waltham, MA, USA). The occludin (Cat#13409), claudin 1 (Cat#13050), zo-1 (Cat#21773) and β-actin (Cat# 20536) antibodies were purchased from Proteintech™ (Wuhan, China). The total antioxidant capacity (T-AOC) assay kit, malondialdehyde (MDA) colorimetric assay kit, catalase (CAT) colorimetric assay kit, and superoxide dismutase (SOD) colorimetric assay kit were purchased from JianCheng Bioengineering Institute (Nanjing, China).

2.2 Animal Studies

The animal studies were approved by the Laboratory Animal Center of Zhejiang Agricultural and Forestry University. Eight weeks old ICR female mice were purchased from Shanghai SLAC Laboratory Animal Company (Shanghai, China), maintained under 12 h light cycle, semi-specific pathogen-free conditions, and fed with autoclaved chow diet. Briefly, after 2 weeks adaptation, mice (n=8 per group) were randomized into 5 groups: Control group (Ctrl), D-galactose treated group (M), D-galactose treated group gavaged with chlorogenic acid (C), D-galactose group gavaged with EGCG (E), and D-galactose group gavaged with chlorogenic acid plus EGCG (C+E). Mice in D-galactose-treated groups were injected intraperitoneally with 200 mg/kg/d D-galactose once per day for totally eight weeks, while mice in the control group were injected with same volume of PBS instead. Mice in C, E, and C+E groups were orally gavaged with 20 mg/kg/d chlorogenic acid (C), 20 mg/kg/d EGCG (E), or 20 mg/kg/d chlorogenic acid plus 20 mg/kg/d EGCG (C+E), dissolved in water, once daily during the whole intervention period. Meanwhile, mice in the Ctrl group or the model group were gavaged with same volume of water. Body weight was measured and recorded every week. Behavior tests were performed during the last week before euthanasia, and fresh feces for microbiota analysis were collected on the last day and stored at -80°C.Following feces collection, mice were fasted 4 h for the gut permeability analysis.

At the end of the experimental period, mice were euthanized, blood was collected by cardiac puncture, and the brain and colon (excluding caecum) tissues were carefully dissected, luminal content removed, and washed with PBS. Then, samples used for RNA extractions was processed immediately, samples used for histochemistry analysis was immersed in 4% (w/v) paraformaldehyde for histochemistry analysis, and the remaining tissues were stored at -80°C.

2.3 Behavior tests

2.3.1 Open field test (OFT)

The OFT was performed as previous described with minor modifications[17]. Mice were placed in the center of a white acrylic box (40cm x 40cm) with grids at the bottom and allowed to move freely for 10 minutes. The behavior and moving path were recorded by a top camera. Crosses mice passed through were calculated. Ethanol (70% v/v) was used to clean all the objects and chamber between trials.

2.3.2 Novel object recognition (NOR)

The NOR test was conducted as previously described with minor modifications[18]. Before testing, mice were placed in an empty open chamber in turns, allowed moving freely and acclimated to the environment for 1 hour on the first day. On the second day, two identical objects (object A) were put at the ends of the chamber opposite to each other. Mice were given 10 minutes to adapt to the objects. On the third day, one of the objects was replaced by a new one (object B), and mice were put inside again for another 10 minutes to explore. The preferential index was calculated using the following formula: Preferential index=Time on object B/(Time on object B+Time on object A)×100%. Ethanol (70% v/v) was used to clean all the objects and chamber between trials.

2.4 Gut permeability analysis and measurement of serum endotoxin

During the last day before euthanasia, mice were fasted for 4h, and then gavaged with fluorescein isothiocyanate conjugated dextran (50 mg per 100 g body weight)[19]. Two hours later, blood was collected and serum was obtained. Fluorescence

intensity (excitation, 490nm; emission, 520nm) in the serum of samples was measured using the Synergy H1 microplate reader (Biotek, VT, USA).

Endotoxemia was determined in serum, according to the manufacturers' instructions (Thermo Fisher Scientific, MA, USA). The absorbance was measured using the Synergy H1 microplate reader (Biotek, VT, USA).

2.5 Histological analysis

After fixing in the 4% paraformaldehyde overnight, colon or brain samples were embedded, with the paraffin embedding machine (EC350, Thermo Fisher Scientific, MA, USA), sliced (4 μm) and stained with the hematoxylin and eosin (H&E). Then once slices were thoroughly dried, samples were observed and representative images at 100x and 400x were taken with the microscopy (BX-41, Olympus, Tokyo, Japan).

2.6 Western Blot

Colon samples were homogenized and lysed with RIPA lysis buffer over ice. The Bradford protein assay kit was used to test the protein content. Protein samples were separated with the 4-12% gradient polyacrylamide gel electrophoresis, and then transferred to the PVDF membranes. After blocking with skim milk for 1 hour, the membranes were incubated with the primary antibody (zo-1, occludin and claudin 1) at 4℃ overnight. β-actin was used as the loading control. After incubation with the secondary antibody (HRP-conjugated; 1:2000 dilution) for 1 h, at room temperature, the conjugates were developed and visualized by the 5200 Multi system (Tanon, Shanghai, China).

2.7 ELISA

Colon samples were homogenized, centrifuged, and then the supernatants were collected. The levels of TNFα, IFN-γ, IL-6 and IL-1β were analyzed according to the manufacturers' instructions (Multisciences Biotech, Hangzhou, China), and normalized by the protein levels tested by Bradford assay. The absorbance was measured using the Synergy H1 microplate reader (Biotek, VT, USA).

2.8 RNA extraction and qRT-PCR analysis

Total RNA of fresh colon or brain samples were extracted using TRIzol™ reagent. The quality and quantity of RNA were analyzed by the Nanodrop™ One spectrophotometer (Thermo Fisher Scientific, MA, USA). Afterwards, cDNA was generated with the ReverTra Ace qPCR RT master mix kit by the Veriti thermal cycler (Thermo Fisher Scientific, MA, USA) and stored in -80 ℃. The cDNA was next mixed with specific primers (Table 1) and SYBR Green Realtime PCR master mix to run the quantitative real-time PCR by the StepOne Realtime PCR system (Thermo Fisher Scientific, MA, USA)[19-21]. Relative mRNA expression levels of specific genes were calculated by the $2^{-\Delta\Delta CT}$ method and β-actin was used as a control.

Table 1. Primer sequences for qRT-PCR analysis

Gene name	Forward (5′-3′)	Reverse (5′-3′)
p16	CGGGGACATCAAGACATCGT	GCCGGATTTAGCTCTGCTCT
p21	CTGTCTTGCACTCTGGTGTCT	CTAAGGCCGAAGATGGGGAA
zo-1	TCTTGCTGGCCCTAAACCTG	GTTGGGCTGGCTCTGAGAAT
occludin	TTCAGGTGAATGGGTCACCG	AGATAAGCGAACCTGCCGAG
claudin 1	TGGGGCTGATCGCAATCTTT	CACTAATGTCGCCAGACCTGA
β-actin	ATGCTCTCCCTCACGCCATC	GAGGAAGAGGATGCGGCAGT

2.9 Redox status analysis

Colon samples were homogenized, centrifuged, and the supernatants were collected. Supernatants were then analyzed with the T-AOC, MDA, CAT, and SOD kits following the manufacturers' instructions (Jiancheng Bioengineering Institute, Nanjing, China). Redox status levels were normalized by the protein levels measured by Bradford assay. The absorbance was measured using the Synergy H1 microplate reader (Biotek, VT, USA).

2.10 Gut microbe 16S rRNA sequencing

Microbial DNA samples were isolated from mouse feces using the E.Z.N.A.® Soil DNA Kit following the manufactures' instructions (Omega Bio-tek, GA, USA). The DNA concentration were quantified using the NanoDrop 2000 UV-vis spectrophotometer (Thermo Fisher Scientific, MA, USA), and DNA quality was checked by 1% agarose gel electrophoresis. Then the V3–V4 regions of bacterial 16S rRNA gene was amplified with universal primers 338 F (5′-ACTCCTACGGGAGGCAGCAG-3′) and 806R (5′-GGACTACHVGGGTWTCTAAT-3′) by ABI GeneAmp® PCR (Thermo Fisher Scientific, MA, USA). Next, the resulted PCR products were extracted from a 2% (w/v) agarose gel and purified using the AxyPrep DNA Gel Extraction Kit (Axygen Biosciences, CA, USA) and quantified using QuantiFluor™-ST (Promega, WI, USA). Purified amplicons were then sequenced by an Illumina MiSeq platform (Illumina, SD, USA) according to the standard protocols by Majorbio Bio-Pharm Technology Co. Ltd. (Shanghai, China).

2.11 Bioinformatic analysis

Raw fastq files were quality-filtered by Trimmomatic and merged by FLASH. Then the high-quality sequences were clustered into operational taxonomic units (OTUs) according to a 97% similarity cutoff using the UPARSE (version 7.1 http://drive5.com/uparse/) with a novel "greedy" algorithm that performs chimera filtering and OTU clustering simultaneously. The taxonomy of each 16S rRNA gene sequence was analyzed by RDP Classifier algorithm (http://rdp.cme.msu.edu/).

2.12 Statistical analysis

Data was summarized as Mean±SD. SPSS (20.0 software, Chicago, IL) was performed to analyze statistical differences among groups by the one-way analysis of variance (ANOVA) and Turkey post hoc tests. p values<0.05 was regarded as being significant different and labeled as *.

For the microbiota analysis, alpha diversity analysis was evaluated with the standard metrics (e.g Chao, Ace, Simpson and Shannon index). The beta diversity analysis was processed by the principal co-ordinates analysis (PCoA) based on the

Bray_Curtis distance metric method. Linear discriminant analysis effect size (LEfSe) analysis was performed with the non-parametric factorial Kruskal-Wallis sum-rank test and linear discriminant analysis (LDA).

3. Results

3.1 Chlorogenic acid and EGCG show no toxicity in D-galactose-induced aging mice.

To evaluate the effect of CGA and EGCG on D-galactose-induced aging mice, we initially assessed body weight progression and food intake every week. At the end of the treatment, the body weight gain of mice treated with D-galactose [the model group (M)] markedly decreased ($p<0.01$), compared with the vehicle treated control group (Figure 1a). While CGA or EGCG, alone, was not able to mitigate the reduction in body weight gain induced by D-galactose, CGA plus EGCG effectively recovered the body weight gain to control level ($p<0.05$). Regarding food intake, the levels of it decreased in all groups in the 2nd week, while it gradually recovered in the following weeks, and no significant differences were observed among groups (Figure 1b).

To determine whether CGA and EGCG treatment affected normal liver function, we assessed the levels of aminotransferases [aspartate aminotransferase (AST) and alanine aminotransferase (ALT)] in serum. After eight weeks of treatment, mice in all groups showed levels of these liver enzymes within the physiological ranges, with no significant differences among groups (Figure 1c).

3.2 Chlorogenic acid in combination with EGCG improves D-galactose-induced cognitive impairment of the aging mice.

We next assessed whether CGA and EGCG could improve the moving and cognitive performance of aging mice (Figure 2a). In the open-field test (OFT), relative to the control group (242 crosses), D-galactose decreased the crossing numbers to 158 crosses ($p<0.05$). While CGA or EGCG alone did not significantly improved on the moving capacity (202 crosses and 180 crosses, respectively), CGA plus EGCG group

effectively recovered the moving ability (271 crosses), being significantly higher than the D-galactose group ($p<0.01$).

Mice in the model group (M) also showed weaker capability on the novel object recognition (NOR), with a preference index of 25.7±8.2%, which was significantly lower than the control group (47.2±3.9%, $p<0.01$). Treatment with EGCG alone or CGA plus EGCG significantly improved the preference index to 45.0±7.1% and 45.7±9.1%, respectively, compared to the D-galactose group($p<0.05$).

Next, we used H&E staining to evaluate the effect of CGA and EGCG on the histopathological changes in the brain after D-galactose in the aging mice (Figure 2b). The morphology of neurons stained with H&E in the control group was normal, with neurons presenting around or oval and clear nucleolus with a regular arrangement. In contrast, the D-galactose-treated group demonstrated severe neuronal changes, such as the presence of dark pycnotic nuclei and a decrease in the cytoplasm. Administration of CGA, EGCG or CGA plus EGCG mitigated this pathologic change (Figure 2b).

Furthermore, D-galactose markedly upregulated the mRNA level of p16 and p21 ($p<0.05$) in the brain, two key age-associated genes, compared with the control group (Figure 2c). CGA and EGCG abrogated the effects of D-galactose on p16 and p21, though no significant difference was observed between D-galactose group and CGA, EGCG groups on p16 expression.

3.3 Chlorogenic acid in combination with EGCG protects the gut barrier of the aging mice.

To assess the effect of CGA and EGCG, alone and in combination, at the gut levels of the aging mice, the colon morphology and gut permeability were evaluated. As shown in Figure 3a, after eight weeks of treatment, D-galactose damaged the colon structure and induced infiltration of lymphocytes in the colon region, which was effectively improved by CGA and EGCG.

In addition, D-galactose severely damaged the gut barrier permeability (Figure 3b). The level of FITC-Dex transport was almost 1.8 times higher in the model group

than in the control group ($p<0.01$). Compared with D-galactose-treated mice, EGCG alone and CGA plus EGCG significantly decreased the gut permeability, recovering the gut permeability to normal levels ($p<0.01$). Consistently, higher level of serum endotoxin was observed in the D-galactose treated group, compared to the control group ($p<0.05$), and supplementation with CGA and EGCG mitigated the increased endotoxin levels induced by D-galactose (Figure 3c).

Tight Junctions (TJs) proteins play pivotal roles in controlling the gut permeability. D-galactose treatment remarkably reduced the protein expression levels of zo-1, occludin and claudin 1, compared to control group ($p<0.01$). While CGA and EGCG alone were unable to restore the levels of zo-1, occludin and claudin 1, the combination of CGA and EGCG effectively restored the levels of these TJs protein expression to similar levels observed in control treated mice (Figure 3d). In agreement, treatment with D-galactose significantly reduced mRNA expression levels of occludin and claudin 1 ($p<0.05$), but not zo-1, which were markedly reversed by C plus E treatment ($p<0.01$; Figure 3e).

3.4 Chlorogenic acid in combination with EGCG reduces D-galactose-induced colon inflammation in aging mice.

We next assessed the effect of C plus E on the gut inflammation induced by D-galactose (Figure 4a). In the model group, D-galactose markedly increased the levels of TNFα and IL-6, compared to the control group ($p<0.05$). While CGA and EGCG alone were unable to suppress TNFα and IL-6 levels, combination of CGA and EGCG significantly reduced TNFα and IL-6 levels, compared to D-galactose alone group ($p<0.05$). Moreover, the level of IFN-γ was enhanced to 3907.8±672.9 pg/mg prot in D-galactose-treated group, whereas EGCG alone and CGA plus EGCG decreased the level to 2829.9±381.3 pg/mg prot ($p<0.05$) and 2308.8±802.4 pg/mg prot ($p<0.01$), respectively. Finally, compared to the control group, D-galactose also increased the levels of the IL-1β to 1182.5±102.9 pg/mg prot ($p<0.01$). C and E both alone or in combination decreased the IL-1β secretion as compared to model group ($p<0.01$).

3.5 Chlorogenic acid in combination with EGCG decreases D-galactose-induced colon oxidative stress in aging mice.

Oxidative stress is another main factor contributing to the enhanced gut permeability. As shown in Figure 4b, compared to control mice, D-galactose significantly decreased the level of total antioxidant capacity (T-AOC) by 29% ($p<0.05$), and induced a 2-fold increase in MDA levels ($p<0.05$). The pro-oxidative effect of D-galactose was reversed by the combination of CGA and EGCG. Aging mice treated with CGA plus EGCG displayed significantly higher level of T-AOC capacity and lower level of MDA compared to D-galactose treated mice ($p<0.05$). Moreover, the activities of catalase (CAT) and superoxide dismutase (SOD) were also reduced ($p<0.05$) in the model group, compared to controls. CGA and EGCG alone partly recovered CAT and SOD activities, whereas CGA plus EGCG greatly increased the SOD activity ($p<0.05$).

3.6 Chlorogenic acid in combination with EGCG improves D-galactose-induced gut dysbiosis in aging mice.

16S rRNA sequencing was performed to evaluate taxa with differential abundance between the aging mice and the ones treated with CGA and EGCG. Compared to the control group, mice in the D-galactose-treated group exhibited overall lower alpha diversity (Figure 5). In the model group, the Shannon index decreased to 3.5 ($p<0.01$) and the Simpson index increased to 0.1 ($p<0.01$), two main factors representing the community diversity. CGA alone recovered the Shannon index to 4.1 ($p<0.05$), and its effect was strengthened when combined with EGCG ($p<0.01$). Similarly, CGA plus EGCG significantly decreased the Simpson index, compared with the model group ($p<0.01$). As the Ace index and Chao index shown, the community richness of aging mice was also decreased, and only C plus E could effectively recover the community richness to the normal level ($p<0.05$).

We next analyzed the species diversity among groups on OTU level. Notably, control and CGA plus EGCG groups shared similarities in PCoA, while the other three groups were quite far away, suggesting that the combination of CGA plus EGCG has a stronger effect in modulating gut dysbiosis than either agent alone (Figure 6a).

Then the community abundance on phylum level and family level were analyzed, respectively. As shown in Figure 6b, compared to the control group, the ratio of Firmicutes, Deferribacter, Actinobacter, and Proteobacter increased, while the ratio of Bacteroidota, Desulfobacte, and Campilobacte decreased in the model group, indicating gut dysbiosis occurred in the aging mice. Compared with the control group, the ratio of Firmicutes/Bacteroidetes in the D-galactose group significantly increased to 3.3±1.6 ($p<0.05$). Both CGA and EGCG positively modulated the gut dysbiosis and showed better effects when combined. The ratio of Firmicutes/Bacteroidetes decreased to 1.0±0.7 in the CGA plus EGCG group, significantly lower than the model group ($p<0.01$). Furthermore, as shown in Figure 6c, the community abundance on family level was further analyzed. Compared to the control group, the level of Lactobacillaceae, Erysipelotrichaceae, Deferribacteraceae, Sutterellaceae, Bifidobacteriaceae, and Eggerthellaceae increased in the model group, while the level of Lachnospiraceae, Muribaculaceae, Rikenellaceae, Bacteroidaceae, and Prevotellaceae decreased. Though CGA and EGCG alone were unable to show a strong effect on D-galactose induced microbiota alteration, CGA plus EGCG greatly affected the microbiota, and the level of Lactobacillaceae was sharply decreased and the ratio of Lachnospiraceae, Muribaculaceae, and Rikenellaceae increased. At the genus level, the top 50 genera with highest community abundance were selected. The relative abundance of dominant genera in the control group and CGA plus EGCG group are relatively similar, while no significant differences were detected among the D-galactose group, CGA group or EGCG group (Figure 6d).

In Figure 7, the dominant microbiota among groups were analyzed by the LEfSe (LDA > 2). In the control group, there are totally 13 prominent features, includes *g_Alistipes* *g_Ruminococcus*, and *g_Anaeroplasma*, whereas c_Bacilli, *o_Lactobacillales*, p_Firmicutes and *o_Enterobacterales*, etc are the 12 specific taxa found in the model group. After CGA plus EGCG treatment, 12 key phylotypes were identified, includes *o_Bacteroidales*, *g_Candidatus_Soleaferrea*, *o_unclassified_c_Clostridia*, *g_unclassfied_f_Anaerovoracaceae*, *g_unclassified_f_Prevotellaceae*, and *g_Tuzzerella*.

4. Discussion

In the present study, we evaluated the anti-aging impact of EGCG and CGA, alone or in combination, with a particular focus on the effect at the gut level. While EGCG and CGA alone partly improve the aging process induced by D-galactose, a significant better effect was observed when these two bioactives were combined.

Cognitive degeneration is a major pathology during aging[3]. In agreement with other studies, the current results showed that chronic administration of D-galactose causes deleterious neuronal damage, which was prevented by CGA and EGCG[22, 23]. Multiple pathways involved in the regulation of aging, particularly, increased expression of p16 and p21 are crucial markers[21]. Though less obvious than brain degeneration, gut also undergoes critical changes during aging with gut permeability increased. Here, D-galactose treatment increased the gut permeability with higher level of serum endotoxin observed. EGCG plus CGA prevented the endotoxemia induced by D-galactose and protected the impaired gut barrier. Mechanistically, TJ proteins connect intercellularly and work as physical barrier in regulating gut permeability[24]. We observed that the combination of CGA and EGCG protected TJs, including zo-1, occludin, and claudin 1, which were damaged by the D-galactose

Aging-dependent gut impairment is linked to chronic oxidative stress, low-grade inflammation and alterations in gut microbiome[25]. Gut highly relies on mitochondrial oxidative phosphorylation (OXPHOS) to meet its high energy requirements, thus it is more susceptible to oxidative injury. Therefore, oxidative stress is widely recognized as the main inductive factor for accelerating gut aging. Due to their antioxidant capacity, CGA and EGCG maintained gut redox balance. Administration of CGA plus EGCG has a stronger effect in attenuating oxidative stress by further increasing the activity of CAT and SOD and decreasing the level of MDA, compared with either agent alone.

Most aged individuals develop a mild proinflammatory state, which is related to increased susceptibility to multiple age-related diseases. The chronic progressive inflammatory process with age was regarded as “inflamm-aging”[26]. Under such a state,

levels of pro-inflammatory cytokines markedly elevate and promote the disruption of gut epithelial barriers[27]. Evidence showed that proinflammatory cytokines TNFα, IFNγ, IL-1β and IL-6 play crucial role in the inflammation amplification cascade, contributing greatly in causing functional opening of TJ barrier[28]. In the present study, D-galactose exposure increased TNFα, IFN-γ, IL-6 and IL-1β levels, which was suppressed by CGA plus EGCG.

Microbiota profile undergoes alterations with increasing age, which affects the gut barrier function and modulates the cognitive capacity through gut-brain axis. In general, Firmicutes and Bacteroidota are the most represented bacteria in all groups, accounting for up to 80% of the total microbiota[29]. The Firmicutes/Bacteroidota ratio evolves during different life stages. Treatment with D-galactose upregulated ratio of Firmicutes/Bacteroidota, which is consistent with other studies[30]. Higher contribution of Deferribacterota was also observed in the D-galactose treated mice, which was positively relevant to gut inflammation[31, 32]. Besides, these shifts were accompanied by an increased prevalence of Actinobacteriota and Proteobacteria, and a reduction in Desulfobacterota in the D-galactose group, which is in line with previous studies[30, 33]. CGA and EGCG reversed the microbial shift induced by D-galactose, and better effect was observed when these two drugs were combined.

At family taxonomic level, treatment with D-galactose increased the level of Lactobacillaceae and decreased the abundance of Lachnospiraceae, and these changes were effectively prevented by CGA plus EGCG. Lactobacillaceae is one of the essential bacteria promotes the growth of secondary bile acids, and highly enriched in the ileum of aging rats[34]. It is observed that Lactobacillaceae could robustly acidify the environment, and inhibit the growth of the commensal gut bacteria, such as Lachnospiraceae and Muribaculaceae (S24-7)[35]. Lachnospiraceae positively modulates the gut barrier integrity and maintains the gut permeability in aged mice[36]. In addition, CGA and EGCG improved the levels of Muribaculaceae, Rikenellaceae, and Bacteroidaceae, which were reduced by D-galactose. Previous studies demonstrated that compared with the young ones, aged mice displayed lower level of Muribaculaceae (S24-7), which is positively associated with gut health and longevity

of mice by producing short chain fatty acids, in particular, propionate[37]. High amount of Rikenellaceae is associated with healthy aging and longevity in Italian elderly, and related with lower risk of metabolic diseases[38]. Moreover, during neonatal dairy calves aging, a decreased abundance of Bacteroidaceae was found to be one of the predominant alterations in the fecal microbiome composition[39]. It is worth noting that CGA plus EGCG treatment protected against the overgrowth of Erysipelotrichaceae and Deferribacteraceae, which are positively correlated with inflammation-related gastrointestinal diseases, such as colorectal cancer, inflammatory bowel disease (IBD) and Crohn's disease (CD)[31, 40]

Moreover, the key phylotypes from phylum to genus of Ctrl, M and C plus E group were identified. c_Bacilli (phylum Firmicutes) was found highly enriched in the model group, and similar results were found in elderly adults[41]. f_Enterobacteriaceae (phylum Proteobacteria) enrichment is frequently coincidence with considerable gut pathology. Patients with inflammatory bowel disease exhibited higher abundance of Enterobacteriaceae, and the outgrowth of Enterobacteriaceae could reversely result in gastrointestinal cell apoptosis and inflammation[42-44]. The abundance of *g_Escherichia-Shigella* was positively correlated with the blood levels of pro-inflammatory cytokines, and could promote the secretion of endotoxins. In CGA plus EGCG supplementation group, *g_Candidatus_Soleaferrea* genus was identified as one of the key taxons possessing anti-inflammatory capacity and maintaining the gut homeostasis[45]. f_Anaerovoracaceae was sparsely characterized, and it was reported to be involved in the gut digestion of plant polyphenols[46]. f_Prevotellaceae enhances SCFAs production, and could protect the gut barrier integrity and improve gut microbiota dysbiosis[47]. In Alzheimer’s disease patients, c_Clostridia and *g_Tuzzerella* were characterized by a decreased amount[48].

5. Conclusion

CGA plus EGCG exerts stronger protective effects against aging related gut barrier impairment than CGA or EGCG alone. After challenged with D-galactose, CGA plus EGCG effectively improved the redox status and mitigated the gut inflammation

damage of the aging mice. Moreover, CGA plus EGCG attenuated the gut homeostasis disturbed by D-galactose, which is characterized by a reduced community diversity and microbiome shift. A limitation of this study is that it evaluated the combined effect of CGA and EGCG against each compound alone at single doses. An important question that remains to be clarified is whether the stronger protective effects against aging-related gut barrier observed with CGA plus EGCG is due to an additive effect between these agents or whether it might be simply due to the presence of higher doses of beneficial compounds at the gut level. Future studies are warranted to elucidate whether CGA and EGCG sensitize each other and whether the combined effect of CGA plus EGCG is superior to a higher dose of the individual compounds. Taken together, these results suggest that the combination of CGA and EGCG is safe and effective in improving the gut barrier function during the aging process.

Conflicts of Interest: The authors declare no conflict of interest.

Acknowledgements: This study was supported by the funds from the Zhejiang Agriculture and Forestry University (2020FR049) and key research and development project of Zhejiang province (2023C04028) to Ran Wei and NIFA-USDA (CA-D-NUT-2397-H) to GGM.

References

1. L. Partridge, J. Deelen and P. E. Slagboom, Facing up to the global challenges of ageing, *Nature*, 2018, **561**, 45-56.
2. P. A. Heidenreich, J. G. Trogdon, O. A. Khavjou, J. Butler, K. Dracup, M. D. Ezekowitz, E. A. Finkelstein, Y. Hong, S. C. Johnston, A. Khera, D. M. Lloyd-Jones, S. A. Nelson, G. Nichol, D. Orenstein, P. W. Wilson, Y. J. Woo, C. American Heart Association Advocacy Coordinating, C. Stroke, R. Council on Cardiovascular, Intervention, C. Council on Clinical, E. Council on, Prevention, A. Council on, Thrombosis, B. Vascular, C. Council on, C. Critical, Perioperative, Resuscitation, N. Council on Cardiovascular, D. Council on the Kidney in Cardiovascular, S. Council on Cardiovascular, Anesthesia, C. Interdisciplinary Council on Quality of and R. Outcomes, Forecasting the future of cardiovascular disease in the United States: a policy statement from the American Heart Association, *Circulation*, 2011, **123**, 933-944.
3. K. F. Azman and R. Zakaria, D-Galactose-induced accelerated aging model: an overview, *Biogerontology*, 2019, **20**, 763-782.
4. T. Takiishi, C. I. M. Fenero and N. O. S. Camara, Intestinal barrier and gut microbiota: Shaping our immune responses throughout life, *Tissue Barriers*, 2017, **5**, e1373208.
5. M. Camilleri, Leaky gut: mechanisms, measurement and clinical implications in humans, *Gut*, 2019, **68**, 1516-1526.
6. Y. R. Li, S. Li and C. C. Lin, Effect of resveratrol and pterostilbene on aging and longevity, *Biofactors*, 2018, **44**, 69-82.
7. N. Khan and H. Mukhtar, Tea polyphenols in promotion of human health, *Nutrients*, 2018, **11**, 39.
8. S. Hayakawa, T. Ohishi, N. Miyoshi, Y. Oishi, Y. Nakamura and M. Isemura, Anti-cancer effects of green tea epigallocatchin-3-gallate and coffee chlorogenic acid, *Molecules*, 2020, **25**, 4553.
9. M. He, L. Zhao, M. J. Wei, W. F. Yao, H. S. Zhao and F. J. Chen, Neuroprotective effects of (-)-epigallocatechin-3-gallate on aging mice induced by D-galactose, *Biol Pharm Bull*, 2009, **32**, 55-60.
10. Y. Hada, H. A. Uchida, N. Otaka, Y. Onishi, S. Okamoto, M. Nishiwaki, R. Takemoto, H. Takeuchi and J. Wada, The Protective Effect of Chlorogenic Acid on Vascular Senescence via the Nrf2/HO-1 Pathway, *Int J Mol Sci*, 2020, **21**, 4527.
11. Y. Feng, Y. H. Yu, S. T. Wang, J. Ren, D. Camer, Y. Z. Hua, Q. Zhang, J. Huang, D. L. Xue, X. F. Zhang, X. F. Huang and Y. Liu, Chlorogenic acid protects D-galactose-induced liver and kidney injury via antioxidation and anti-inflammation effects in mice, *Pharm Biol*, 2016, **54**, 1027-1034.
12. N. Yamamoto, H. Tokuda, G. Kuroyanagi, S. Kainuma, R. Ohguchi, K. Fujita, R. Matsushima-Nishiwaki, O. Kozawa and T. Otsuka, Amplification by (-)-epigallocatechin gallate and chlorogenic acid of TNF-alpha-stimulated interleukin-6 synthesis in osteoblasts, *Int J Mol Med*, 2015, **36**, 1707-1712.
13. L. Yang, L. Jia, X. Li, K. Zhang, X. Wang, Y. He, M. Hao, M. P. Rayman and J.

Zhang, Prooxidant activity-based guideline for a beneficial combination of (-)-epigallocatechin-3-gallate and chlorogenic acid, *Food Chem*, 2022, **386**, 132812.
14. A. Ali, S. A. Shah, N. Zaman, M. N. Uddin, W. Khan, A. Ali, M. Riaz and A. Kamil, Vitamin D exerts neuroprotection via SIRT1/nrf-2/ NF-kB signaling pathways against D-galactose-induced memory impairment in adult mice, *Neurochem Int*, 2021, **142**, 104893.
15. T. Shwe, W. Pratchayasakul, N. Chattipakorn and S. C. Chattipakorn, Role of D-galactose-induced brain aging and its potential used for therapeutic interventions, *Exp Gerontol*, 2018, **101**, 13-36.
16. Z. Ma, F. Zhang, H. Ma, X. Chen, J. Yang, Y. Yang, X. Yang, X. Tian, Q. Yu, Z. Ma and X. Zhou, Effects of different types and doses of whey protein on the physiological and intestinal flora in D-galactose induced aging mice, *PLoS One*, 2021, **16**, e0248329.
17. J. Kang, Z. Wang, E. Cremonini, G. Le Gall, M. G. Pontifex, M. Muller, D. Vauzour and P. I. Oteiza, (-)-Epicatechin mitigates anxiety-related behavior in a mouse model of high fat diet-induced obesity, *J Nutr Biochem*, 2022, **110**, 109158.
18. Z. Wu, T. Chen, D. Pan, X. Zeng, Y. Guo and G. Zhao, Resveratrol and organic selenium-rich fermented milk reduces D-galactose-induced cognitive dysfunction in mice, *Food Funct*, 2021, **12**, 1318-1326.
19. R. Wei, X. Liu, Y. Wang, J. Dong, F. Wu, G. G. Mackenzie and Z. Su, (-)-Epigallocatechin-3-gallate mitigates cyclophosphamide-induced intestinal injury by modulating the tight junctions, inflammation and dysbiosis in mice, *Food Funct*, 2021, **12**, 11671-11685.
20. J. Wang, H. Zhao, K. Lv, W. Zhao, N. Zhang, F. Yang, X. Wen, X. Jiang, J. Tian, X. Liu, C. T. Ho and S. Li, Pterostilbene ameliorates DSS-induced intestinal epithelial barrier loss in mice via suppression of the NF-kappaB-mediated MLCK-MLC signaling pathway, *J Agric Food Chem*, 2021, **69**, 3871-3878.
21. J. Qian, X. Wang, J. Cao, W. Zhang, C. Lu and X. Chen, Dihydromyricetin attenuates D-galactose-induced brain aging of mice via inhibiting oxidative stress and neuroinflammation, *Neurosci Lett*, 2021, **756**, 135963.
22. J. Liu, D. Chen, Z. Wang, C. Chen, D. Ning and S. Zhao, Protective effect of walnut on d-galactose-induced aging mouse model, *Food Sci Nutr*, 2019, **7**, 969-976.
23. E. Hakimizadeh, M. Zamanian, L. Gimenez-Llort, C. Sciorati, M. Nikbakhtzadeh, M. Kujawska, A. Kaeidi, J. Hassanshahi and I. Fatemi, Calcium dobesilate reverses cognitive deficits and anxiety-like behaviors in the D-galactose-induced aging mouse model through modulation of oxidative stress, *Antioxidants (Basel)*, 2021, **10**, 649.
24. R. Okumura and K. Takeda, Roles of intestinal epithelial cells in the maintenance of gut homeostasis, *Exp Mol Med*, 2017, **49**, e338.
25. T. Finkel and N. J. Holbrook, Oxidants, oxidative stress and the biology of ageing, *Nature*, 2000, **408**, 239-247.

26. M. G. Flynn, M. M. Markofski and A. E. Carrillo, Elevated inflammatory status and increased risk of chronic disease in chronological aging: inflamm-aging or inflamm-inactivity?, *Aging Dis*, 2019, **10**, 147-156.
27. A. C. Luissint, C. A. Parkos and A. Nusrat, Inflammation and the intestinal barrier: leukocyte-epithelial cell interactions, cell junction remodeling, and mucosal repair, *Gastroenterology*, 2016, **151**, 616-632.
28. G. Barbara, M. R. Barbaro, D. Fuschi, M. Palombo, F. Falangone, C. Cremon, G. Marasco and V. Stanghellini, Inflammatory and microbiota-related regulation of the intestinal epithelial barrier, *Front Nutr*, 2021, **8**, 718356.
29. M. Serino, E. Luche, S. Gres, A. Baylac, M. Berge, C. Cenac, A. Waget, P. Klopp, J. Iacovoni, C. Klopp, J. Mariette, O. Bouchez, J. Lluch, F. Ouarne, P. Monsan, P. Valet, C. Roques, J. Amar, A. Bouloumie, V. Theodorou and R. Burcelin, Metabolic adaptation to a high-fat diet is associated with a change in the gut microbiota, *Gut*, 2012, **61**, 543-553.
30. K. A. Kim, J. J. Jeong, S. Y. Yoo and D. H. Kim, Gut microbiota lipopolysaccharide accelerates inflamm-aging in mice, *BMC Microbiol*, 2016, **16**, 9.
31. H. Zhang, Z. Zhang, G. Song, X. Tang, H. Song, A. Deng, W. Wang, L. Wu and H. Qin, Development of an XBP1 agonist, HLJ2, as a potential therapeutic agent for ulcerative colitis, *Eur J Pharm Sci*, 2017, **109**, 56-64.
32. O. I. Selmin, A. J. Papoutsis, S. Hazan, C. Smith, N. Greenfield, M. G. Donovan, S. N. Wren, T. C. Doetschman, J. M. Snider, A. J. Snider, S. H. Chow and D. F. Romagnolo, n-6 high fat diet induces gut microbiome dysbiosis and colonic inflammation, *Int J Mol Sci*, 2021, **22**, 6919.
33. G. Leite, M. Pimentel, G. M. Barlow, C. Chang, A. Hosseini, J. J. Wang, G. Parodi, R. Sedighi, A. Rezaie and R. Mathur, Age and the aging process significantly alter the small bowel microbiome, *Cell Rep*, 2021, **36**, 109765.
34. S. M. Lee, N. Kim, J. H. Park, R. H. Nam, K. Yoon and D. H. Lee, Comparative analysis of ileal and cecal microbiota in aged rats, *J Cancer Prev*, 2018, **23**, 70-76.
35. E. J. E. Brownlie, D. Chaharlangi, E. O. Wong, D. Kim and W. W. Navarre, Acids produced by lactobacilli inhibit the growth of commensal Lachnospiraceae and S24-7 bacteria, *Gut Microbes*, 2022, **14**, 2046452.
36. S. Hu, J. Wang, Y. Xu, H. Yang, J. Wang, C. Xue, X. Yan and L. Su, Anti-inflammation effects of fucosylated chondroitin sulphate from Acaudina molpadioides by altering gut microbiota in obese mice, *Food Funct*, 2019, **10**, 1736-1746.
37. M. Sibai, E. Altuntas, B. Yildirim, G. Ozturk, S. Yildirim and T. Demircan, Microbiome and longevity: high abundance of longevity-linked Muribaculaceae in the gut of the long-living rodent spalax leucodon, *OMICS*, 2020, **24**, 592-601.
38. T. Tavella, S. Rampelli, G. Guidarelli, A. Bazzocchi, C. Gasperini, E. Pujos-Guillot, B. Comte, M. Barone, E. Biagi, M. Candela, C. Nicoletti, F. Kadi, G. Battista, S. Salvioli, P. W. O'Toole, C. Franceschi, P. Brigidi, S. Turroni and A. Santoro, Elevated gut microbiome abundance of Christensenellaceae,

Porphyromonadaceae and Rikenellaceae is associated with reduced visceral adipose tissue and healthier metabolic profile in Italian elderly, *Gut Microbes*, 2021, **13**, 1-19.
39. E. T. Kim, S. J. Lee, T. Y. Kim, H. G. Lee, R. M. Atikur, B. H. Gu, D. H. Kim, B. Y. Park, J. K. Son and M. H. Kim, Dynamic changes in fecal microbial communities of neonatal dairy calves by aging and diarrhea, *Animals (Basel)*, 2021, **11**, 1113.
40. W. Turpin, L. Bedrani, O. Espin-Garcia, W. Xu, M. S. Silverberg, M. I. Smith, J. A. R. Garay, S. H. Lee, D. S. Guttman, A. Griffiths, P. Moayyedi, R. Panaccione, H. Huynh, H. A. Steinhart, G. Aumais, L. A. Dieleman, D. Turner, C. I. G. P. r. team, A. D. Paterson and K. Croitoru, Associations of NOD2 polymorphisms with Erysipelotrichaceae in stool of in healthy first degree relatives of Crohn's disease subjects, *BMC Med Genet*, 2020, **21**, 204.
41. E. Biagi, L. Nylund, M. Candela, R. Ostan, L. Bucci, E. Pini, J. Nikkila, D. Monti, R. Satokari, C. Franceschi, P. Brigidi and W. De Vos, Through ageing, and beyond: gut microbiota and inflammatory status in seniors and centenarians, *PLoS One*, 2010, **5**, e10667.
42. C. J. Anderson, C. B. Medina, B. J. Barron, L. Karvelyte, T. L. Aaes, I. Lambertz, J. S. A. Perry, P. Mehrotra, A. Goncalves, K. Lemeire, G. Blancke, V. Andries, F. Ghazavi, A. Martens, G. van Loo, L. Vereecke, P. Vandenabeele and K. S. Ravichandran, Microbes exploit death-induced nutrient release by gut epithelial cells, *Nature*, 2021, **596**, 262-267.
43. K. M. Chasser, K. McGovern, A. F. Duff, B. D. Graham, W. N. Briggs, D. R. Rodrigues, M. Trombetta, E. Winson and L. R. Bielke, Evaluation of day of hatch exposure to various Enterobacteriaceae on inducing gastrointestinal inflammation in chicks through two weeks of age, *Poultry Sci*, 2021, **100**, 101193.
44. D. N. Frank, A. L. St Amand, R. A. Feldman, E. C. Boedeker, N. Harpaz and N. R. Pace, Molecular-phylogenetic characterization of microbial community imbalances in human inflammatory bowel diseases, *Proc Natl Acad Sci U S A*, 2007, **104**, 13780-13785.
45. J. Cai, L. Zhou, X. D. Song, M. Q. Yin, G. Q. Liang, H. Xu, L. R. Zhang, G. R. Jiang and F. Huang, Alteration of intestinal microbiota in 3-Deoxyglucosone-induced prediabetic rats, *Biomed Res Int*, 2020, **2020**, 8406846.
46. C. L. Shen, R. Wang, G. C. Ji, M. M. Elmassry, M. Zabet-Moghaddam, H. Vellers, A. N. Hamood, X. X. Gong, P. Mirzaei, S. M. Sang and V. Neugebauer, Dietary supplementation of gingerols- and shogaols-enriched ginger root extract attenuate pain-associated behaviors while modulating gut microbiota and metabolites in rats with spinal nerve ligation, *Journal of Nutritional Biochemistry*, 2022, **100**, 108904.
47. C. Khoo, C. Duysburgh, M. Marzorati, P. Van den Abbeele and D. Zhang, A freeze-dried cranberry powder consistently enhances SCFA production and lowers abundance of opportunistic pathogens in vitro, *BioTech (Basel)*, 2022, **11**, 14.

48. A. Kaiyrlykyzy, S. Kozhakhmetov, D. Babenko, G. Zholdasbekova, D. Alzhanova, F. Olzhayev, A. Baibulatova, A. R. Kushugulova and S. Askarova, Study of gut microbiota alterations in Alzheimer's dementia patients from Kazakhstan, *Sci Rep*, 2022, **12**, 15115.

Figure legends

Figure 1. Effect of CGA (C) and EGCG (E) on body weight, food intake and hepatic functions in D-galactose (M) treated mice. (a) Body weight progression. Treatment with CGA (C) and EGCG (E) mitigated the body weight loss induced by D-galactose (M). Results are presented as mean±SD. *p<0.05, **p<0.01 vs. control. (b) Weekly food intake. Results are presented as mean±SD. (c) Serum levels of Alanine

aminotransferase (ALT) and Aspartate aminotransferase (AST) at euthanasia. Results are presented as mean±SD.

Figure 2. Effect of CGA (C) and EGCG (E), alone and in combination, on the cognitive performance of mice treated with D-galactose (M). (a) Behavior was evaluated by the open field test (OFT) and the novel object recognition test (NOR). D-galactose-treated mice (M) reduced cognitive behavior, which was mitigated by CGA (C) plus EGCG (E). Results are presented as mean±SD. *p<0.05, **p<0.01 vs. control. (b) Representative Hematoxylin and Eosin (H&E) histology images of the brain at euthanasia for all experimental groups. Images at 100x (top) and 400x (bottom) magnification are displayed. (c) Effect of C and E on p16 and p21 mRNA expression in D-galactose (M)-treated mice brains. Results are presented as mean±SD. *p<0.05, **p<0.01 vs. control.

Figure 3. CGA (C) and EGCG (E) protected the gut barrier of the mice injured by D-galactose (M) treatment. (a) CGA (C) and EGCG (E) ameliorated the inflammatory cell infiltration induced by D-galactose (M) in colon tissue. Representative H&E histology images of colon tissue at euthanasia for all experimental groups. Images at 40x (top) and 100x (bottom) magnification are displayed. (b) C and E reduced the gut permeability, measured by the fluorescein isothiocyanate-dextran (FITC-Dextran) transport. Results are presented as mean±SD. *p<0.05, **p<0.01 vs. control. (c) C and E reduced serum endotoxin levels induced by D-galactose. (d) C

plus E restored the decrease in tight junction protein expression induced by D-galactose (M) in colon tissue. Immunoblots for zo-1, occludin, and claudin 1 are shown. Loading control: β-actin. Bands were quantified and results are presented as percentage of control. *p<0.05 and **p<0.01 vs. control. (e) Effect of C and E on colon zo-1, occludin, and claudin 1 mRNA expression in D-galactose (M) treated mice. Results are presented as mean±SD. *p<0.05 and **p<0.01 vs. control.

Figure 4. Effect of CGA (C) plus EGCG (E) on inflammation and gut oxidative stress in D-galactose (M) treated mice. (a) Levels of TNFα, IFN-γ, IL-1β, and IL-6 in colon tissues. Results were normalized by protein contents and presented as mean±SD. *p<0.05, **p<0.01 vs. control. (b) Levels of total antioxidant capacity (T-AOC), malondialdehyde (MDA), and activity of catalase (CAT) and superoxide dismutase (SOD) in colon tissues. Results were normalized by the protein contents and presented as mean±SD. *p<0.05, **p<0.01 vs. control.

Figure 5. Effect of CGA (C) and EGCG (E) on the α-diversity of the fecal microbiome in mice treated with D-galactose (M). Shannon, Simpson, Ace and Chao 1 indexes were determined in Control (Ctrl), D-galactose (M), CGA (C), EGCG (E), and CGA plus EGCG (C+E) groups to evaluate the gut microbiota community diversity and richness among groups. *p<0.05; **p<0.01.

Figure 6. Effect of CGA (C) and EGCG (E) on fecal microbiota composition in

mice treated with D-galactose (M). (a) Principal component analysis (PCA) and principal coordinates analysis (PCoA) of the community structure. (b) Gut microbiota distribution at the phylum level and the Firmicutes/Bacteroidetes ratio. (c) Gut microbiota distribution at the family level. (d) Community heatmap of relative abundance at the genus level.

Figure 7. Linear discriminant analysis effect size (LEfSe) analysis on fecal microbiome of the mice treated with D-galactose (M). Bacterial taxa with linear discriminant analysis (LDA) score>2 specifically enriched in control (Ctrl; red), D-galactose-treated mice (M; blue) and CGA (C) and EGCG (E) (CE; purple) groups.

Figure 1

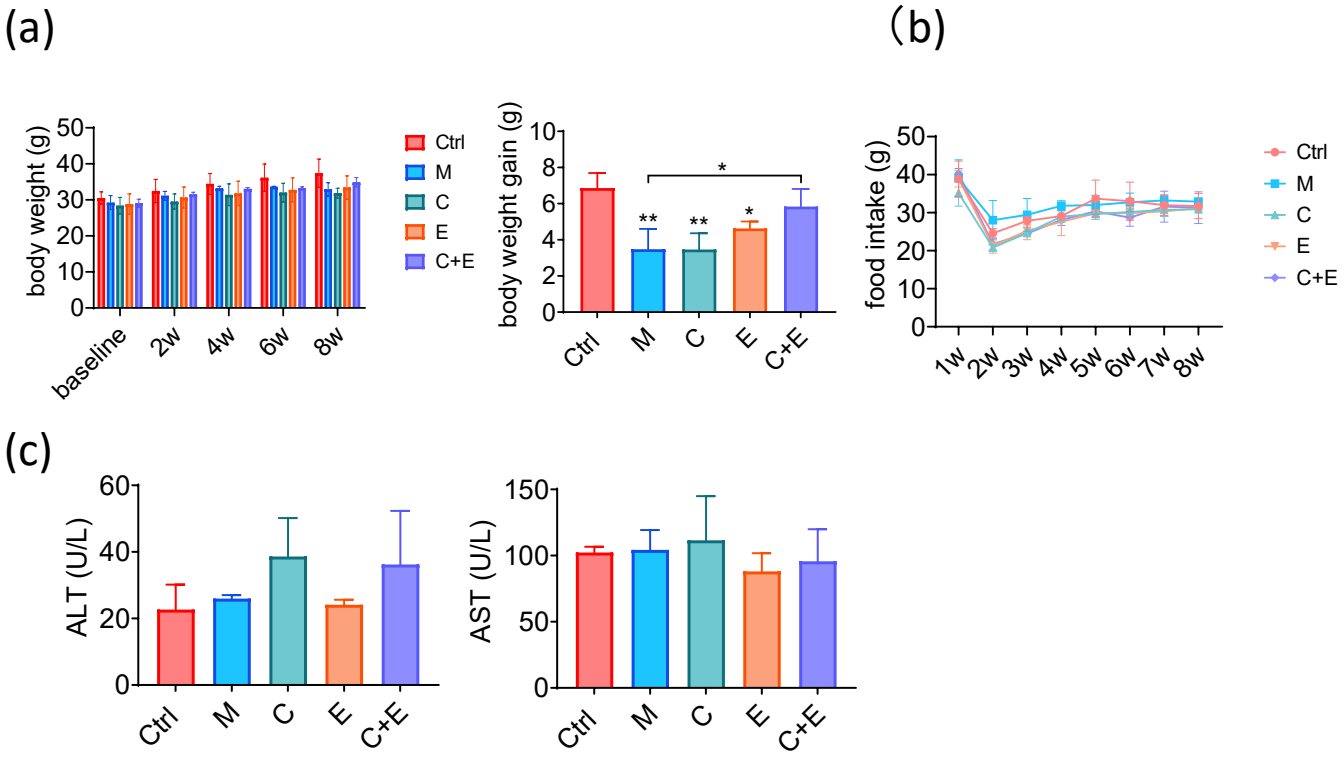
(a)
body weight (g)
baseline
2w
4w
6w
8w
Ctrl
M
C
E
C+E
body weight gain (g)
**
**
*
*
(b)
food intake (g)
1w
2w
3w
4w
5w
6w
7w
8w
(c)
ALT (U/L)
AST (U/L)

Figure 2

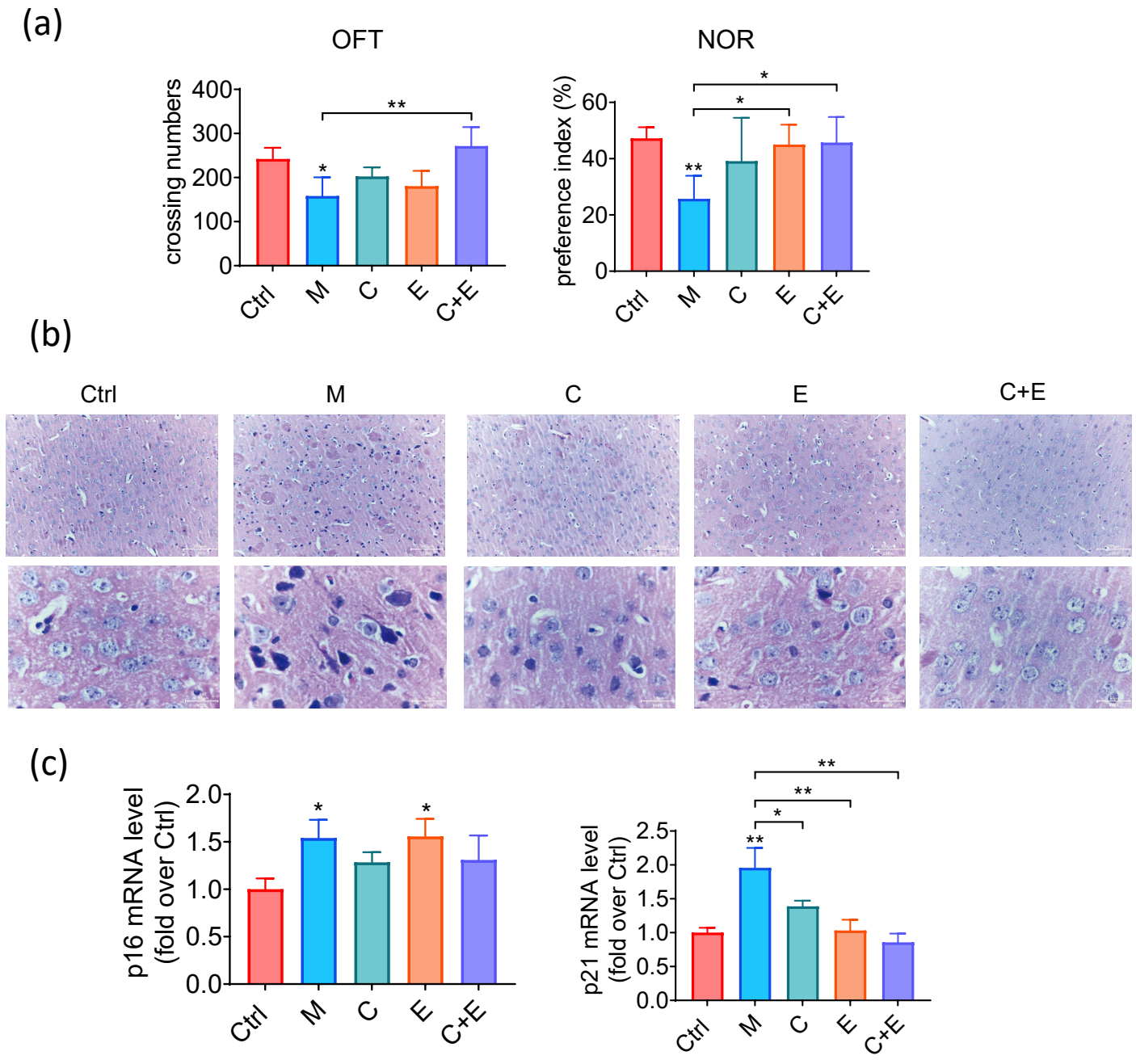
(a)
OFT
NOR
crossing numbers
preference index (%)
Ctrl
M
C
E
C+E
(b)
Ctrl
M
C
E
C+E
(c)
p16 mRNA level (fold over Ctrl)
p21 mRNA level (fold over Ctrl)

Figure 3

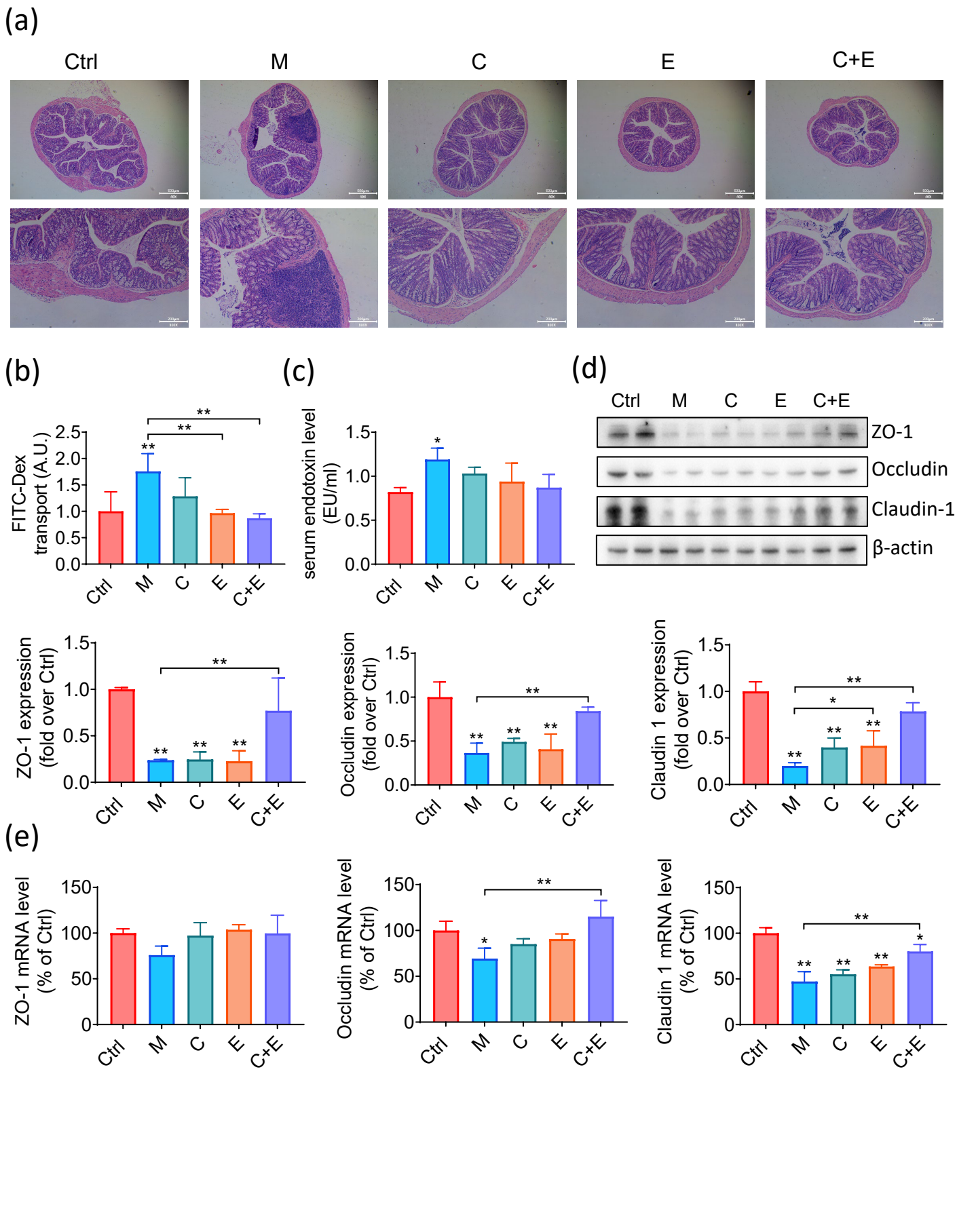
(a)
Ctrl
M
C
E
C+E
(b)
FITC-Dex transport (A.U.)
(c)
serum endotoxin level (EU/ml)
(d)
Ctrl M C E C+E
ZO-1
Occludin
Claudin-1
β-actin
ZO-1 expression (fold over Ctrl)
Occludin expression (fold over Ctrl)
Claudin 1 expression (fold over Ctrl)
(e)
ZO-1 mRNA level (% of Ctrl)
Occludin mRNA level (% of Ctrl)
Claudin 1 mRNA level (% of Ctrl)

Figure 4

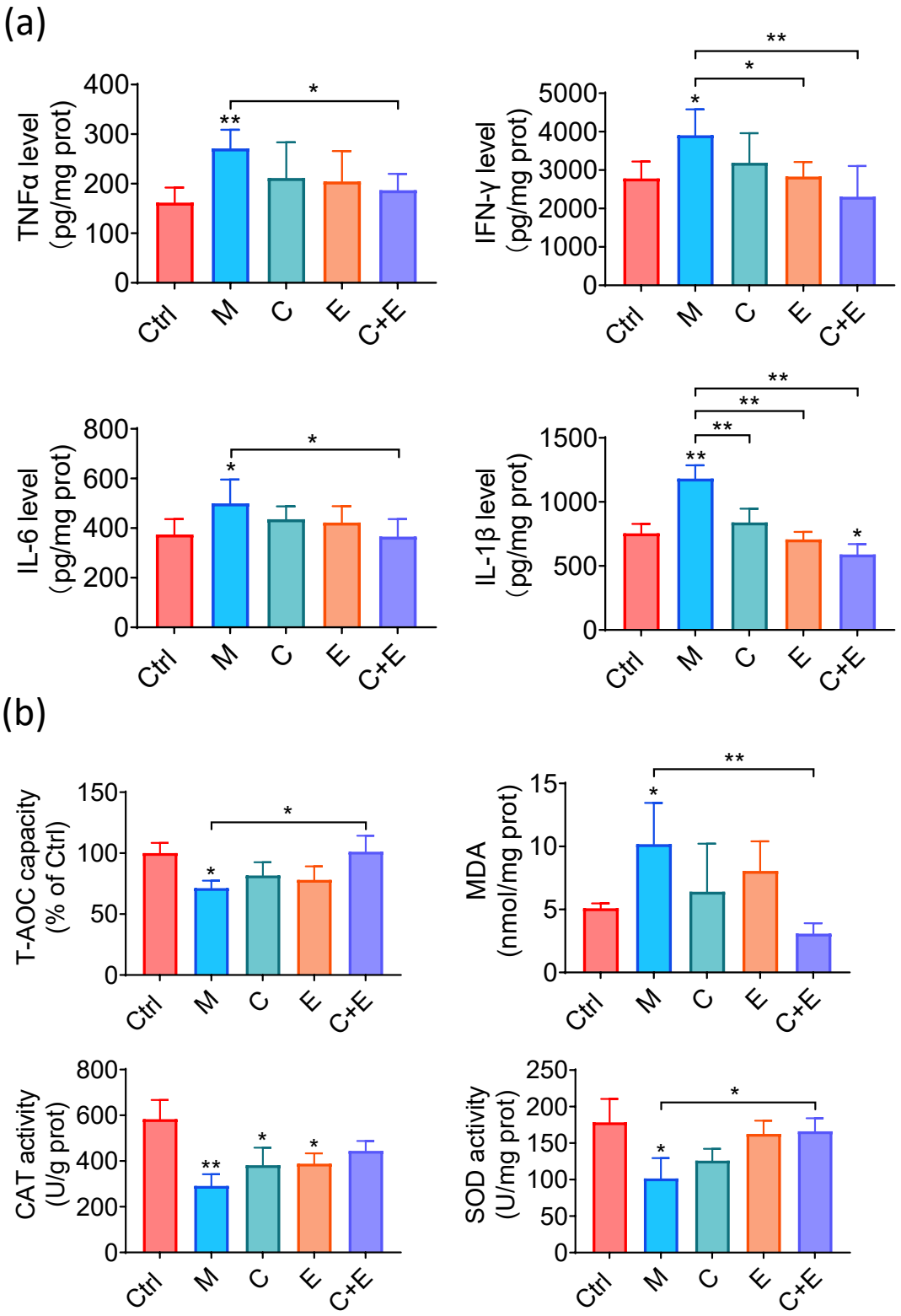
(a)
TNFα level (pg/mg prot)
IFN-γ level (pg/mg prot)
IL-6 level (pg/mg prot)
IL-1β level (pg/mg prot)
(b)
T-AOC capacity (% of Ctrl)
MDA (nmol/mg prot)
CAT activity (U/g prot)
SOD activity (U/mg prot)
Ctrl
M
C
E
C+E

Figure 5

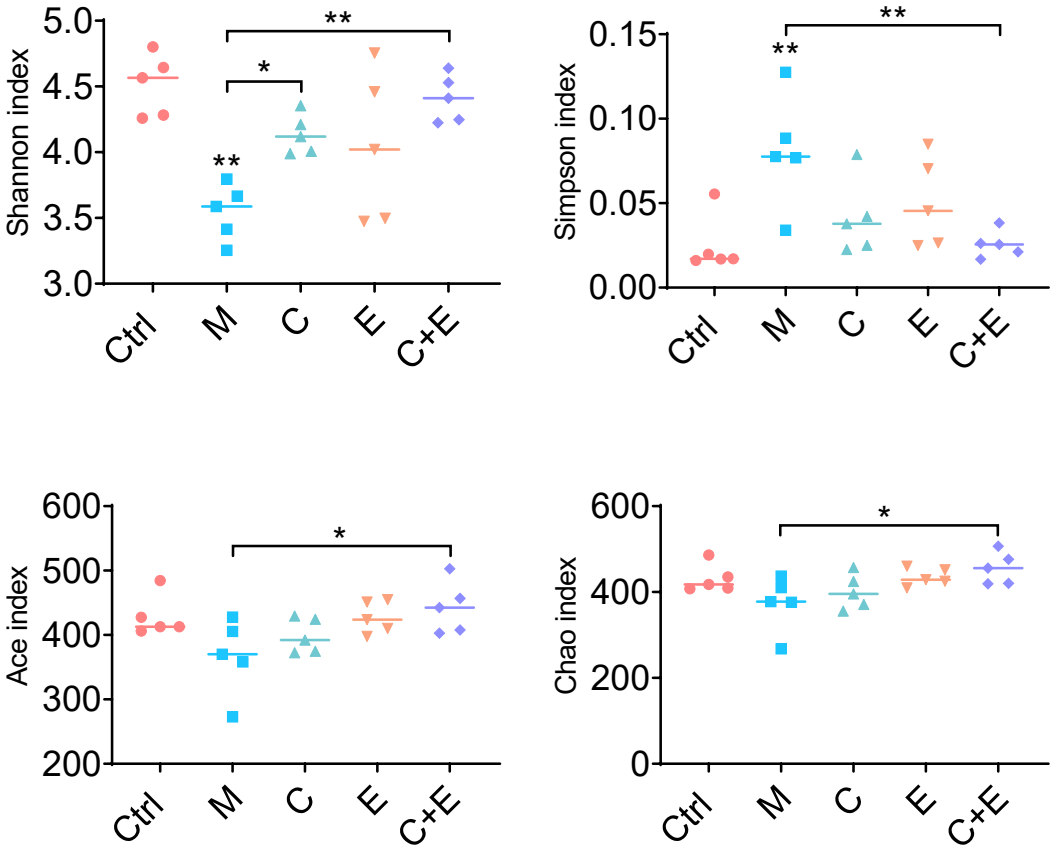
Shannon index
5.0
4.5
4.0
3.5
3.0
**
*
**
Ctrl
M
C
E
C+E
Simpson index
0.15
0.10
0.05
0.00
**
**
Ctrl
M
C
E
C+E
Ace index
600
500
400
300
200
*
Ctrl
M
C
E
C+E
Chao index
600
400
200
0
*
Ctrl
M
C
E
C+E

Figure 6

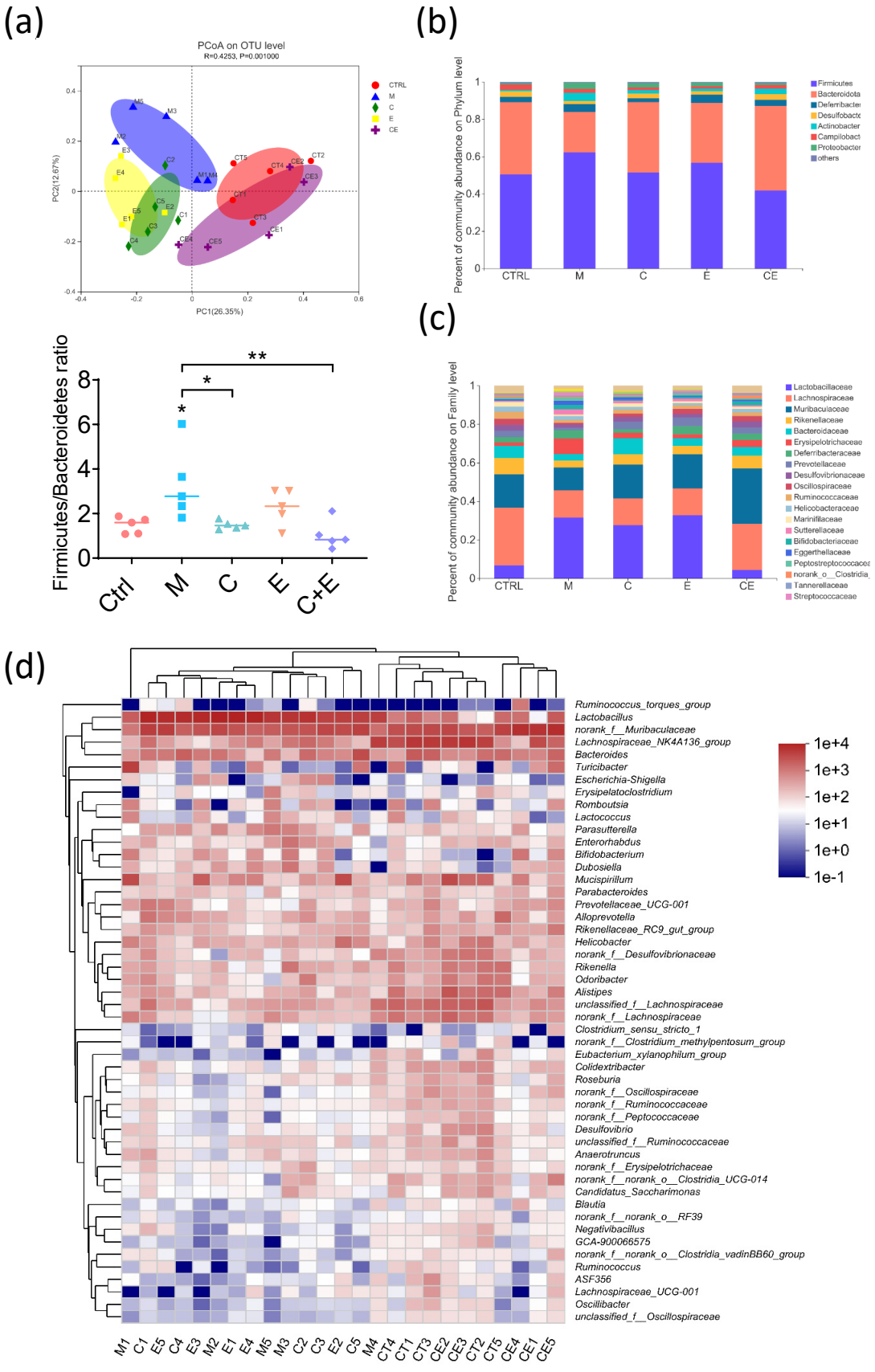
(a)
PCoA on OTU level
R=0.4253, P=0.001000
PC1(26.35%)
PC2(12.67%)
CTRL
M
C
E
CE
(b)
Percent of community abundance on Phylum level
Firmicutes
Bacteroidota
Deferribacte
Desulfobacte
Actinobacter
Campilobact
Proteobacter
others
CTRL
M
C
E
CE
(c)
Firmicutes/Bacteroidetes ratio
Ctrl
M
C
E
C+E
Percent of community abundance on Family level
Lactobacillaceae
Lachnospiraceae
Muribaculaceae
Rikenellaceae
Bacteroidaceae
Erysipelotrichaceae
Deferribacteraceae
Prevotellaceae
Desulfovibrionaceae
Oscillospiraceae
Ruminococcaceae
Helicobacteraceae
Marinifilaceae
Sutterellaceae
Bifidobacteriaceae
Eggerthellaceae
Peptostreptococcacea
norank_o__Clostridia_
Tannerellaceae
Streptococcaceae
(d)
Ruminococcus_torques_group
Lactobacillus
norank_f__Muribaculaceae
Lachnospiraceae_NK4A136_group
Bacteroides
Turicibacter
Escherichia-Shigella
Erysipelatoclostridium
Romboutsia
Lactococcus
Parasutterella
Enterorhabdus
Bifidobacterium
Dubosiella
Mucispirillum
Parabacteroides
Prevotellaceae_UCG-001
Alloprevotella
Rikenellaceae_RC9_gut_group
Helicobacter
norank_f__Desulfovibrionaceae
Rikenella
Odoribacter
Alistipes
unclassified_f__Lachnospiraceae
norank_f__Lachnospiraceae
Clostridium_sensu_stricto_1
norank_f__Clostridium_methylpentosum_group
Eubacterium_xylanophilum_group
Colidextribacter
Roseburia
norank_f__Oscillospiraceae
norank_f__Ruminococcaceae
norank_f__Peptococcaceae
Desulfovibrio
unclassified_f__Ruminococcaceae
Anaerotruncus
norank_f__Erysipelotrichaceae
norank_f__norank_o__Clostridia_UCG-014
Candidatus_Saccharimonas
Blautia
norank_f__norank_o__RF39
Negativibacillus
GCA-900066575
norank_f__norank_o__Clostridia_vadinBB60_group
Ruminococcus
ASF356
Lachnospiraceae_UCG-001
Oscillibacter
unclassified_f__Oscillospiraceae
1e+4
1e+3
1e+2
1e+1
1e+0
1e-1
M1 C1 E5 C4 E3 M2 E1 E4 M5 M3 C2 C3 E2 C5 M4 CT4 CT1 CT3 CE2 CE3 CT2 CT5 CE4 CE1 CE5

Figure 7

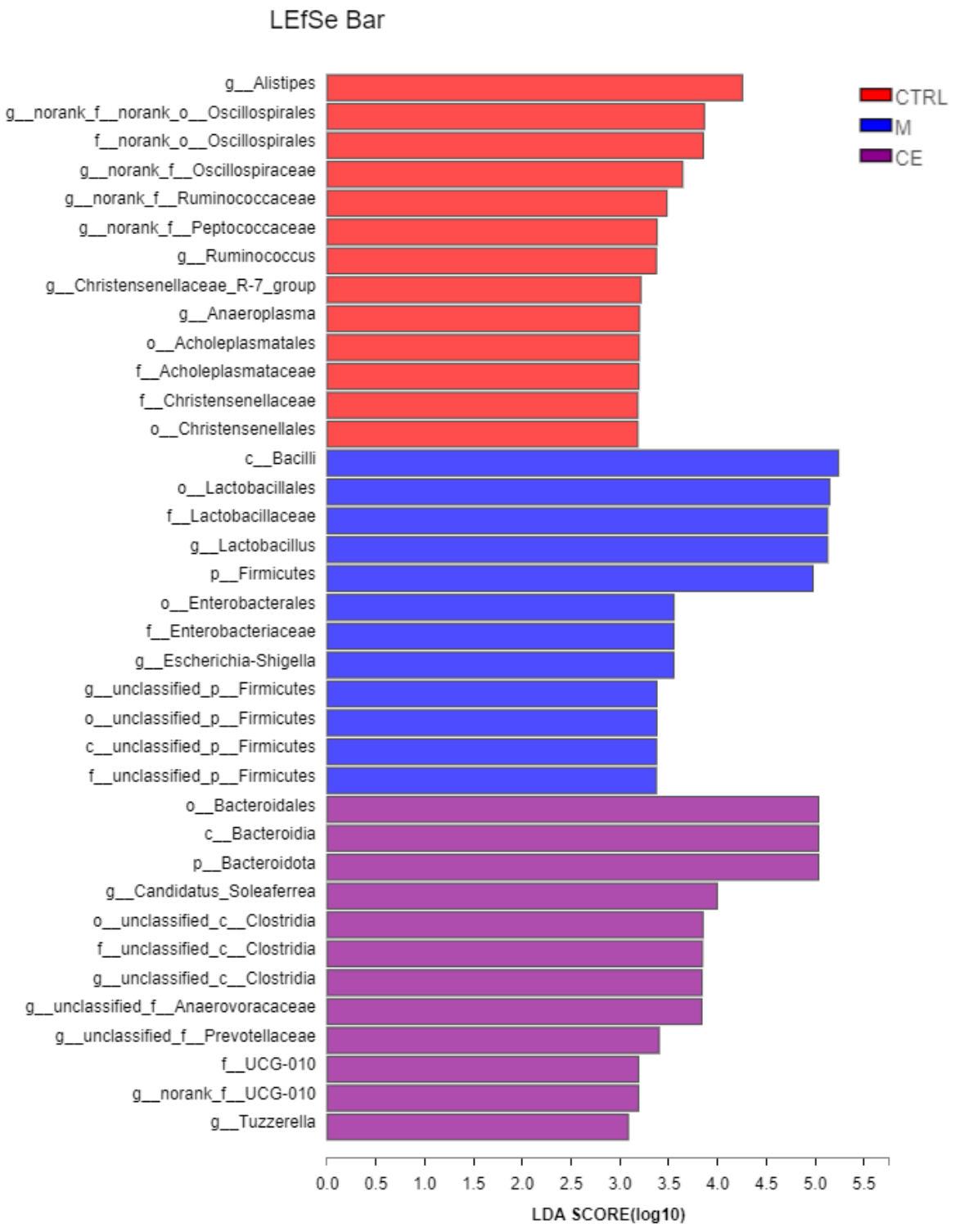
LEfSe Bar
g__Alistipes
g__norank_f__norank_o__Oscillospirales
f__norank_o__Oscillospirales
g__norank_f__Oscillospiraceae
g__norank_f__Ruminococcaceae
g__norank_f__Peptococcaceae
g__Ruminococcus
g__Christensenellaceae_R-7_group
g__Anaeroplasma
o__Acholeplasmatales
f__Acholeplasmataceae
f__Christensenellaceae
o__Christensenellales
c__Bacilli
o__Lactobacillales
f__Lactobacillaceae
g__Lactobacillus
p__Firmicutes
o__Enterobacterales
f__Enterobacteriaceae
g__Escherichia-Shigella
g__unclassified_p__Firmicutes
o__unclassified_p__Firmicutes
c__unclassified_p__Firmicutes
f__unclassified_p__Firmicutes
o__Bacteroidales
c__Bacteroidia
p__Bacteroidota
g__Candidatus_Soleaferrea
o__unclassified_c__Clostridia
f__unclassified_c__Clostridia
g__unclassified_c__Clostridia
g__unclassified_f__Anaerovoracaceae
g__unclassified_f__Prevotellaceae
f__UCG-010
g__norank_f__UCG-010
g__Tuzzerella
CTRL
M
CE
0.0 0.5 1.0 1.5 2.0 2.5 3.0 3.5 4.0 4.5 5.0 5.5
LDA SCORE(log10)

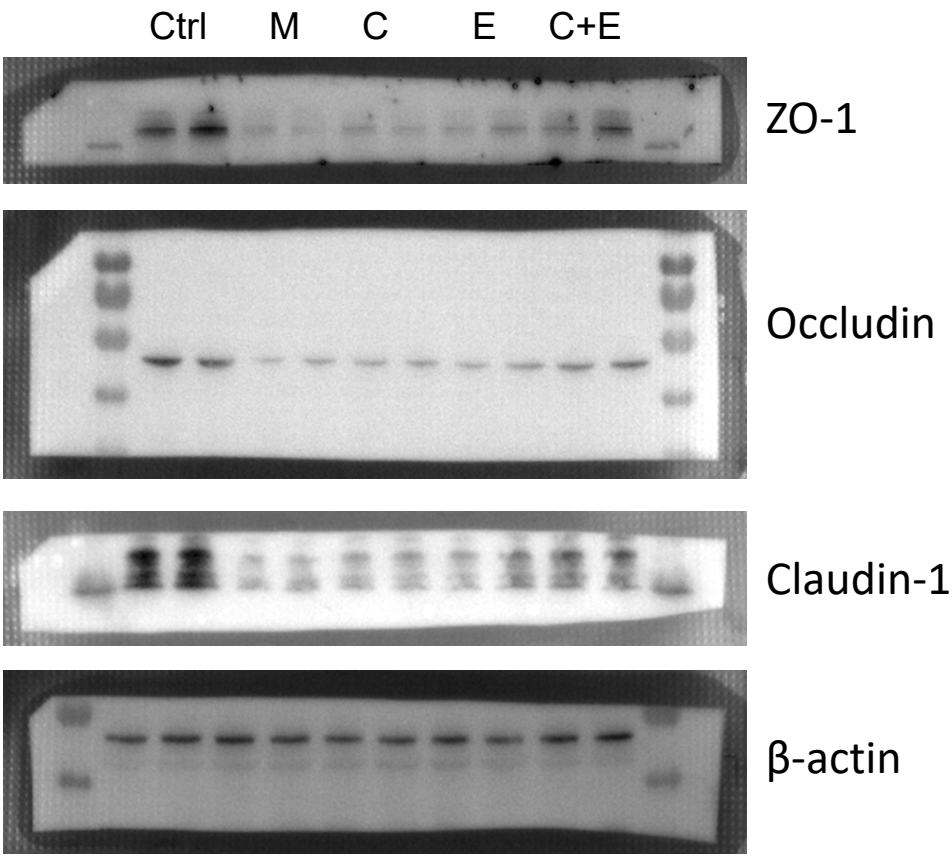
Ctrl
M
C
E
C+E
ZO-1
Occludin
Claudin-1
β-actin